Oncogenic role of miR-17-92 cluster in anaplastic thyroid cancer cells

Shu Takakura[1], Norisato Mitsutake[1], Masahiro Nakashima[2], Hiroyuki Namba[1], Vladimir A. Saenko[3], Tatiana I. Rogounovitch[1], Yuka Nakazawa[1], Tomayoshi Hayashi[4], Akira Ohtsuru[5] , and Shunichi Yamashita[1, 3, 5]

[1]Department of Molecular Medicine, [2]Tissue and Histopathology Section, Division of Scientific Data Registry, [3]Department of International Health and Radiation Research, Atomic Bomb Disease Institute, Nagasaki University Graduate School of Biomedical Sciences, 1-12-4 Sakamoto, Nagasaki 852-8523, Japan

[4]Department of Pathology, [5]Takashi Nagai Memorial International Hibakusha Medical Center, Nagasaki University Hospital of Medicine and Dentistry, 1-7-1 Sakamoto, Nagasaki 852-8501, Japan

Running title: miR-17-92 in anaplastic thyroid cancer

Key words: Anaplastic thyroid cancer, miRNA, miR-17-92 cluster, miR-17-3p, miR-17-5p, miR-19a

Correspondence:

Norisato Mitsutake, MD PhD

Department of Molecular Medicine, Atomic Bomb Disease Institute

Nagasaki University Graduate School of Biomedical Sciences

1-12-4 Sakamoto, Nagasaki 852-8523, Japan

Tel: +81-95-819-7116, Fax: +81-95-819-7117

E-mail: mitsu@nagasaki-u.ac.jp

This work was supported in part by Grant-in-Aid for Scientific Research (#18790637 and #18591030) and Global COE Program from the Ministry of Education, Culture, Sports, Science and Technology of Japan, the President's discretionary fund of Nagasaki University and Nagasaki Igakudousoukai fund for medical research.

Summary

Micro RNAs (miRNAs) are non-coding small RNAs and constitute a novel class of negative gene regulators that are found in both plants and animals. Several miRNAs play crucial roles in cancer cell growth. To identify miRNAs specifically deregulated in anaplastic thyroid cancer (ATC) cells, we performed a comprehensive analysis of miRNA expressions in ARO cells and primary thyrocytes using miRNA microarrays. miRNAs in miR-17-92 cluster were over-expressed in ARO cells. We confirmed the over-expression of those miRNAs by Northern blot in ARO and FRO cells. In 3 of 6 clinical ATC samples, miR-17-3p and miR-17-5p were robustly over-expressed in cancer lesion compared to adjacent normal tissue. To investigate the functional role of these miRNAs in ATC cells, ARO and FRO cells were transfected with miRNA inhibitors, antisense oligonucleotides containing locked nucleic acids. Suppression of miR-17-3p caused complete growth arrest, presumably due to caspase activation resulting in apoptosis. miR-17-5p or miR-19a inhibitor also induced strong growth reduction, but only miR-17-5p inhibitor led to cellular senescence. On the other hand, miR-18a inhibitor only moderately attenuated the cell growth. Thus, we have clarified functional differences among the members of the cluster in ATC cells. In conclusion, these findings suggest that the mir-17-92 cluster plays an important role in certain types of ATCs and could be a novel target for ATC treatment.

Introduction

MicroRNAs (miRNAs) are non-coding, single-stranded small RNAs and constitute a novel class of gene regulators that are found in both plants and animals [(1)]. Mature miRNAs, ranging from 18 to 25 nucleotides in length, processed by two-step cleavage involving Drosha and Dicer are thought to negatively regulate messenger RNA (mRNA). The mature miRNA binds to target mRNA and induces its cleavage or translational repression depending on the degree of complementarity [(2)]. Although hundreds of miRNAs have been already cloned, only a small number of them have been characterized.

Recently, several miRNAs have been reported to be involved in cell proliferation or apoptosis in various types of cancers [(3, 4)]. miR-15a and miR-16 induce apoptosis by targeting BCL2, and these miRNAs are frequently deleted or under-expressed in chronic lymphocytic leukemia [(5)]. let-7 expression is reduced in lung cancer with poor prognosis [(6)] and inversely correlates with expression of RAS protein, suggesting a possible mechanism for cancer cell proliferation [(7)]. Compared to these under-expressed miRNAs, miR-21 has an anti-apoptotic function and is over-expressed in glioblastoma. Knockdown of miR-21 in glioblastoma cells induced caspase activation, resulting in apoptotic cell death [(8)]. Thus, miRNAs can act as both tumor suppressor and oncogene.

The miR-17-92 cluster, composed of seven miRNAs (miR-17-5p, miR-17-3p, miR-18a,

miR-19a, miR-20a, miR-19b and miR-92-1) and located in intron 3 of the *C13orf25* gene, is over-expressed in lung cancer and B-cell lymphoma [9, 10]. Enforced expression of truncated cluster comprising miR-17-5p~19b (miR-17-19b), the vertebrate-specific portion of the miR-17-92 cluster, accelerated tumor development in mouse B-cell lymphoma model, suggesting oncogenic function of miR-17-19b. On the other hand, O'Donnell et al. have reported that expression of oncogenic E2F1 is negatively regulated by miR-17-5p and miR-20a, members of the cluster, implying that they act as a tumor suppressor [11]. Thus, the function of the cluster is still controversial.

In thyroid cancer, over-expression of several miRNAs has been reported. He et al. have reported that three miRNAs (miR-221, miR-222 and miR-146) are over-expressed in papillary thyroid carcinomas (PTCs) and regulate KIT expression [12]. Another group has also shown that miR-221, miR-222 and miR-181b are over-expressed in PTCs, and inhibition of miR-221 by antisense oligonucleotides led to attenuation of cell growth [13]. In follicular thyroid cancers (FTCs), miR-197 and miR-346 are significantly over-expressed [14]. *In vitro* over-expression of either miRNA induced cell proliferation, whereas inhibition led to growth arrest. Very recently, Visone et al. have reported that significant decrease in miR-30d, miR-125b, miR-26a and miR-30a-5p was detected in human anaplastic thyroid cancers (ATCs) [15].

ATCs are highly aggressive and fatal tumors with less than eight months of mean survival after diagnosis [16]. Various treatment patterns including radiation and

chemotherapy have been tried in ATCs, but they are mostly unsuccessful [17]. Therefore, the identification of miRNAs involved in proliferation or apoptosis in ATC cells has important therapeutic implications and may lead to establishment of a novel therapy for ATCs. In the present study, we show that mir-17-92 cluster, which is over-expressed in ARO and FRO cells, has a crucial role in cell growth and survival. These findings suggest that the mir-17-92 cluster might be a novel target for ATC treatment.

Materials and Methods

Cell culture. We used ATC cell lines ARO, FRO [18] and KTC-2 (derived from anaplastic transformed PTC) [19]; PTC cell lines NPA and TPC-1 [20]; FTC cell line WRO [21]; and PT. All cells used in this study are of human origin. ARO, FRO, NPA and WRO were kindly provided by Dr. G. Juillard (University of California, Los Angels, CA, USA). TPC-1 and KTC-2 were kindly provided by Dr. Sato (Cancer Institute, Kanazawa University, Kanazawa, Japan) and Dr. Kurebayashi (Kawasaki Medical School, Kurashiki, Japan), respectively. All cells (except PT) were maintained in RPMI-1640 medium supplemented with 5% fetal bovine serum (FBS) and penicillin/streptomycin at 37ºC in a humidified atmosphere with 5% CO_2. PT were isolated from thyroid tissues obtained during subtotal thyroidectomy in patients with Graves' disease and cultured as described previously [22]. All experiments were performed after obtaining hospital ethical committee approval. Informed consent was

obtained from each individual.

miRNA microarray. Small RNAs (~200 nt) were extracted from ARO cells and PT using a mirVana miRNA Isolation Kit (Ambion, Austin, TX, USA). Five micrograms of the small RNAs were subjected to Custom microRNA Array Analysis Service (http://www.hssnet.co.jp/e/2/2_4_5_1.html) (Hokkaido System Science, Sapporo, Japan). The array contained 313 oligonucleotide probes for mature miRNA.

Northern blot analysis. Total RNA was extracted from cells using ISOGEN reagent (Nippon Gene, Tokyo, Japan). Ten micrograms of total RNA were separated on 15% denaturing polyacrylamide gel and electrotransferred onto Nylon Membrane Positively Charged (Roche Diagnostics, Basel, Switzerland). Oligonucleotides complementary to mature miRNAs were labeled with digoxigenin by terminal transferase-mediated 3' end-labeling and used as probes. The sequences of oligonucleotides were as follows: miR-17-5p, 5'-actacctgcactgtaagcactttg-3'; miR-17-3p, 5'-acaagtgccttcactgcagt-3'; miR-18a, 5'-tatctgcactagatgcacctta3'; miR-19a, 5'-tcagttttgcatagatttgcaca-3'; miR-19b, 5'-tcagttttgcatggatttgcaca-3'; miR-20a, 5'-ctacctgcactataagcacttta-3'; miR-92-1, 5'-caggccgggacaagtgcaata-3'; miR-21, 5'-tcaacatcagtctgataagcta-3'; let-7, 5'-gaggtagtaggttgtatagtt-3'; miR-106a, 5'-gctacctgcactgtaagcactttt-3'; miR-106b, 5'-atctgcactgtcagcacttta-3'; 5S-rRNA, 5'-ttagcttccgagatcagacga-3'. The membrane was then hybridized with hybridization mixture (0.25 M Na_2HPO_4, pH 7.2/1 mM EDTA/1% BSA/7% SDS/15% formamide and the labeled probes) overnight at 43 or 45ºC. After

hybridization, the membrane was washed with wash mixture (20 mM Na_2HPO_4, pH 7.2/1 mM EDTA/1% SDS) followed by washing buffer (0.1 M maleic acid/0.15 M NaCl/0.3% Tween-20). After blocking with 1% Blocking Reagent (Roche Diagnostics), the hybridized membrane was incubated with alkaline phosphatase-conjugated anti-DIG antibody (Roche Diagnostics). The membrane was then washed with the washing buffer. After equilibration with detection buffer (0.1 M Tris-HCl pH 9.5/0.1 M NaCl), the membrane was incubated with chemiluminescent substrate CDP Star (Roche Diagnostics). Detection was performed using a LAS3000 imaging system (FUJIFILM, Tokyo, Japan). After detection, the membrane was stripped and used for re-hybridization a few times.

Real-time reverse transcription (RT) – polymerase chain reaction (PCR). The quantitative real-time RT-PCR for miRNA was performed using TaqMan MicroRNA Assay System (Applied Biosystems, Foster City, CA, USA). Briefly, 10 ng of total RNA was reverse transcribed using looped RT primer which is specific for each miRNA. The following amplification was performed using a corresponding TaqMan MicroRNA Assay Mix (Applied Biosystems) in a Thermal Cycler Dice Real-time System (Takara Bio Inc., Ohtsu, Japan). The cycle threshold value, which was determined using second derivative, was used to calculate the normalized expression of the indicated miRNAs using Q-Gene software [23].

RNA isolation from human ATC samples. Human ATC tissues and adjacent normal

thyroid tissues were dissected from 6 formalin-fixed paraffin-embedded (FFPE) surgically resected samples. Total RNA was extracted using RecoverAll Total Nucleic Acid Isolation Kit for FFPE (Ambion) according to the manufacturer's protocol. Briefly, tissues were collected in microcentrifuge tubes from sections thicker than 20 μm and deparaffinized with 100% xylene followed by washing twice with 100% ethanol. Each sample was then digested with protease at 50ºC for 3 hr. For RNA isolation, sample solution was passed through filter cartridge provided by manufacturer, and then DNase treatment was performed on the filter at room temperature for 30 minutes. After washing several times with washing solution, total RNA was eluted with heated nuclease free water.

Oligonucleotide transfection for suppression of endogenous miRNA. Locked nucleic acid (LNA) and deoxyribo nucleic acid (DNA) hybrid (LNA/DNA) antisense oligonucleotides (miR inhibitors) were chemically synthesized by Greiner Bio-one (Frickenhausen, Germany). The miR inhibitors contained LNAs at eight consecutive centrally located bases (indicated by capital letters) as described previously (12). The sequences of the inhibitors were as follows: LNA-17-5p, 5'-actacctgCACTGTAAgcactttg-3'; LNA-17-3p, 5'-acaagtGCCTTCACtgcagt; LNA-18a, 5'-tatctgcACTAGATGcacctta-3'; LNA-19a, 5'-tcagtttTGCATAGAtttgcaca-3'; LNA-21, 5'-tcaacatCAGTCTCTGAtaagcta-3'. Transfection was done using Lipofectamine 2000 reagent (Invitrogen, Carlsbad, CA, USA).

Growth Curves. Cells (ARO: 3 x 10^4; FRO: 1 x 10^4 cells) were plated in each well of 24-well plates. Twelve hours later, the cells were transfected with miR inhibitors (first transfection). Second transfection was done at 48 hr after first transfection. At indicated times, the cells were detached by trypsinization, and the cell number was counted using a hemocytometer.

Imaging of Caspase Activation. Cells were incubated with 5 μM DRAQ5 (Biostatus Limited, Leicestershire, UK) for 10 minutes followed by 25 μM D2R (Rhodamine 110 bis-L-aspartic acid amide) (Invitrogen Molecular Probes) for 15 minutes at 37ºC. Cell images were obtained using a LSM510 META confocal microscope (Carl Zeiss, Oberkochen, Germany).

Senescence-associated β-galactosidase (SA-β-gal) staining. Cells were fixed with 2% formaldehyde/0.2% glutalaldehyde and assayed for SA-β-gal activity using X-gal (5-bromo-4-chloro-3-indolyl β-D-galactosidase) at pH 6.0 as described previously [24, 25]. SA-β-gal-positive cells were detected by bright-field microscopy. The percentages of positive cells were determined by scoring approximately 200-400 cells/field for each sample.

Western blot analysis. Cells were lysed in a buffer containing 20 mM Tris-HCl (pH 7.5), 1 mM EDTA, 150 mM NaCl, 0.5% Triton-X, 2 mM phenylmethylsulfonyl fluoride,

50 mM sodium fluoride, 10 mM sodium pyrophosphate, 1 mM sodium orthovanadate, 5% glycerol and Complete protease inhibitor cocktail (Roche Diagnositics). Equal amount of protein was separated by SDS-PAGE and transferred onto nitrocellulose membrane Bio Trace (Pall Corporation, Pensacola, FL, USA). The following primary antibodies were used: anti-PARP (Cell Signaling Technology, Beverly, MA, USA), anti-caspase 9 (Cell Signaling Technology), anti-caspase 3 (Cell Signaling Technology), anti-RB 4H1 (Cell Signaling Technology), anti-PTEN A2B1 (Santa Cruz Biotechnology, Santa Cruz, CA, USA) and anti-β-actin C4 (Santa Cruz Biotechnology). The antigen-antibody complexes were visualized using horseradish peroxidase-conjugated anti-mouse or anti-rabbit IgG antibody (Cell Signaling Technology) and Chemi-Lumi One system (Nacalai Tesque, Kyoto, Japan). The image was obtained using a LAS3000 imaging system (FUJIFILM).

DNA agarose gel electrophoresis. Genomic DNA was extracted from the pellets used for protein extraction. The pellets were incubated with 500 μl TEN buffer containing 40 mM Tris-HCl (pH 8.0), 1 mM EDTA, 150 mM NaCl and proteinase K at 55ºC overnight. Then, DNA was extracted using phenol/chloroform/isoamylalcohol method and ethanol precipitation. Four hundred ng of DNA was electrophoretically separated on 1.5% agarose gel. Ethidium bromide was used for staining and the image was obtained using a UV transilluminator.

Statistical analysis. Differences between groups were examined for statistical

significance using one-way analysis of variance (ANOVA) followed by Fisher's PLSD. P value not exceeding 0.05 was considered statistically significant.

Results

Distinct miRNA expression pattern in ATC cells. To identify miRNAs specifically deregulated in ATC cells, we performed a comprehensive analysis of miRNA expression in ARO cells and PT using miRNA microarrays. Seven percent of miRNAs were over-expressed (> 2.0-fold) and 7% were under-expressed (< 0.5-fold) in ARO cells compared to PT. Fold changes of representative miRNAs expression are listed in Table 1. All members of miR-17-92 cluster except miR-17-3p were over-expressed in ARO cells. With respect to cancer-related miRNAs, miR-16 was over-expressed, and let-7 and miR-21 were expressed at almost normal level.

Over-expression of miRNAs in miR-17-92 cluster in thyroid cancer cell lines. Next, we performed Northern blotting to confirm the microarray data and also to check the expressions of several miRNAs in various thyroid cancer cell lines. All members of the miR-17-92 cluster (miR-17-5p, miR-17-3p, miR-18a, miR-19a, miR-20a, miR-19b and miR-92-1) were robustly over-expressed in ATC cell lines, ARO and FRO (Fig. 1A). We also examined some other cancer-related miRNAs. As shown in Fig. 1B, let-7 and miR-21 were expressed at normal to slightly lower level. In ARO cells, the results of

Northern blotting were mostly consistent with the microarray data.

miR-106a and miR-106b have high homologous sequence to miR-17-5p (please see Fig. 3C), raising the possibility that signals detected with the miR-17-5p probe on Northern blot were caused by cross-hybridization to miR-106a and miR-106b. We thus utilized TaqMan real-time RT-PCR assay that is basically capable of discriminating single mismatched nucleotide [26]. As shown in Fig. 1C, not only miR-17-5p but also miR-106a and miR-106b were over-expressed in ARO cells. We also observed over-expression of miR-17-3p which has no homologous miRNA, leading to the conclusion that the miR-17-92 cluster was *bona fide* over-expressed in ARO cells (Fig. 1C).

Over-expression of miR-17-3p and miR-17-5p in human ATC samples. We next analyzed expression levels of miR-17-3p and miR-17-5p in clinical human ATC samples and paired adjacent normal tissue. TaqMan real-time RT-PCR assay was also used in this experiment. In 3 of 6 cases, those miRNAs were robustly over-expressed in ATC lesions compared to normal portions (Fig. 2). Two cases showed decreased expression in ATC lesions, and one case showed no change. This result suggests that the miR-17-92 cluster is over-expressed in some types of ATCs and may have a role in ATC pathogenesis.

miR inhibitors abolish endogenous miRNA expressions. The miR-17-92 cluster has been reported to be over-expressed in certain types of cancers; however, the function of each individual miRNA in the cluster is still controversial. Since

miR-17-19b is vertebrate-specific portion of the miR-17-92 cluster and has been reported to sufficiently act as an oncogene in mouse B cell lymphoma model [9], we focused in greater detail on miRNAs in miR-17-19b. To explore biological significance of the members of miR-17-19b, ARO cells were transfected with corresponding miR inhibitor for the each member. Transfection efficiency was initially assessed using FITC-conjugated DNA oligonucleotides and fluorescence microscope, and it was almost 100% in our hands (data not shown). Since miRNA can bind to target mRNA with imperfect match, we used cells treated with transfection reagent only as a control instead of using scrambled oligonucleotides to avoid any unpredictable effects. We then checked specificity of each miR inhibitor by Northern blotting. As shown in Fig. 3A, target miRNAs became undetectable up to 48 hr after transfection and the effect was sequence-specific. However, at 72 hr after transfection, the target miRNA expression was slightly restored (data not shown). In addition, miR-20a, which has a similar sequence to miR-17-5p (2-base difference, Fig. 3C), and miR-19b, similar to miR-19a (1-base difference, Fig. 3C), were also undetectable in cells transfected with LNA-17-5p and LNA-19a, respectively (Fig. 3B). Moreover, expression of miR-106a and miR-106b, which also have a homologous sequence to miR-17-5p (2-base and 3-base difference, respectively, Fig. 3C), were similarly affected by LNA-17-5p (Fig. 3B). Considering that probes for miR-106a and miR-106b probably detect all of miR-17-5p, miR-20a, miR-106a and miR-106b, LNA-17-5p seemed to block all of those miRNAs. On the other hand, the expression of miR-18a, which also shares some homology with miR-17-5p (6-base difference, Fig. 3C), was not altered by LNA-17-5p

(Fig. 3A). Similarly, miR-20a expression was not affected with LNA-18a (4-base difference, Fig. 3B and 3C).

Effects of inhibition of endogenous miRNA on ARO and FRO cell growth. We next investigated the effect of inhibition of the members of miR-17-19b on ARO and FRO cell growth. As shown in Fig. 4A and 4B, LNA-17-3p totally suppressed the cell growth, and many detached cells were also observed (data not shown). LNA-17-5p and LNA-19a also dramatically inhibited the growth (Fig. 4A and 4B). In contrast to LNA-17-3p, detached cells were barely detected with these miR inhibitors (data not shown). On the other hand, the growth reduction by LNA-18a was moderate, and LNA-21 did not affect at all (Fig. 4A and 4B). In ARO cells, LNA-17-5p, LNA-17-3p, LNA-18a and LNA-19a suppressed the growth in a dose-dependent fashion, and the inhibitory effect by LNA-17-3p at lower concentration (e.g. 10 pmol/well) was far greater than that of any other miR inhibitors (Fig. 4C).

LNA-17-3p induces apoptosis. Since cell detachments were exclusively observed in cells transfected with LNA-17-3p, we next explored the mechanism of growth inhibition by each miR inhibitor. We first investigated caspase activation using D2R substrate after transfection with miR inhibitors. D2R is a cell-permeable nonfluorescent derivative of rhodamine 110. Upon enzymatic cleavage by caspases, this substrate is converted into fluorescent rhodamine 110, enabling us to measure the caspase activity in living cells. Cells were simultaneously stained with DRAQ-5 to evaluate nuclear

morphology. As shown in Fig. 5A, intense activation of caspases was found only in the cells transfected with LNA-17-3p. Nuclear apoptotic changes, such as fragmentation or chromatin condensation, were also observed (Fig. 5A, arrowheads). Despite the significant growth reduction by LNA-17-5p or LNA-19a (Fig. 4), there was no caspase activation in cells with those inhibitors (Fig. 5A). We then performed Western blotting to check the activation of caspase 3 and 9, key mediators of apoptosis. As shown in Fig. 5B, both caspases were most clearly activated by LNA-17-3p. LNA-17-3p also caused cleavage of PARP (Fig.5B) and DNA fragmentation (Fig. 5C), supporting the evidence of apoptosis induced by LNA-17-3p.

LNA-17-5p induces cell senescence. We then examined SA-β-gal activity in ARO cells transfected with miR inhibitors. Senescent and/or terminally differentiated cells are known to show enlarged granular phenotype and to possess SA-β-gal activity at pH 6.0 [(24)]. As shown in Fig. 6A and 6B, the number of SA-β-gal-positive and enlarged cells was significantly increased in cells treated with LNA-17-5p but not with LNA-17-3p or LNA-19a. This finding suggests that one of the mechanisms of growth inhibition by LNA-17-5p is senescence-like growth arrest.

LNA-17-5p and LNA-19a induce expression of retinoblastoma protein 1 (RB1) and PTEN, respectively. To explore further mechanisms of the growth arrest by LNA-17-5p and LNA-19a, we also checked protein expression of tumor suppressors RB1 and PTEN after transfecion with those miR inhibitors. RB1 and PTEN have been

predicted to be targets of miR-17-5p (miR-20a, miR-106a and miR-106b) and miR-19a (miR-19b), respectively [27]. As shown in Fig. 7, the expression of RB1 and PTEN was clearly increased in cells transfected with LNA-17-5p and LNA-19a, respectively.

Discussion

The miR-17-92 cluster located on the *C13orf25* gene has been reported to act as an oncogene in cooperation with MYC in B-cell lymphoma [9]. On the other hand, O'Donnell et al. have reported that MYC directly binds to the cluster locus and regulates the transcription of miR-17-92 pri-miRNA. miR-17-5p and miR-20a, members of the miR-17-92 cluster, negatively regulate the expression of E2F1 which promotes cell cycle progression. This finding suggests that these miRNAs have a tumor suppressor activity [11]. These two studies seem to contradict each other. However, E2F1 is reported to induce apoptosis when the level of this protein is excessive [28]. Since MYC also directly induces E2F1 transcription, this mechanism may be present to achieve efficient cell proliferation by tightly regulating the E2F1 expression. Thus, the overall consequence of over-expressing miR-17-92 cluster probably depends on cellular environment and level of target mRNA expression.

In the present work, we have shown the clear over-expression of miRNAs in the miR-17-92 cluster in ATC cell lines and some of the clinical ATC cases. We have also

revealed their growth-promoting effects using miR inhibitors. Contrary to our findings, Visone et al. have recently reported that no miR was over-expressed in 10 human ATC samples using microarray technique [15]. This discrepancy could be due to their method of analysis in which mean of fold change was calculated and cutoff of two-fold was applied. In addition, it is generally observed that differences in expression level measured by microarray are usually smaller (underestimated) than actual differences. Our results suggest that at least in some of ATC cases the miR-17-92 cluster play a role. However, mechanism of regulating the cluster in each case remains to be explored.

Inhibition of miR-17-3p caused apoptosis with caspase activation. Interestingly, the massive caspase activation was not observed in cells transfected with any other miR inhibitors. miR-17-3p clearly has a distinct function from other members of the cluster. To our knowledge, however, there is no report regarding target mRNA of miR-17-3p. Further studies are required to clarify the function of miR-17-3p in ATCs.

Although LNA-17-5p and LNA-19a induced relatively strong growth reduction, only LNA-17-5p caused some degree of cellular senescence in ARO cells. Lazzerini Denchi et al. have proposed the model in which sustained E2F activity induces cellular senescence, whereas temporal E2F activation evokes cell proliferation [29]. Because MYC is over-expressed in ARO cells compared to PT [30], inhibition of miR-17-5p and miR-20a by LNA-17-5p might cause prolonged E2F1 activation which results in cellular senescence. However, further investigation is required to clarify the detailed

mechanism.

One of predicted targets for miR-19a and miR-19b is tumor suppressor PTEN [31]. As expected, definite up-regulation of PTEN was observed in ARO cells transfected with LNA-19a, suggesting that one of targets of miR-19a and miR-19b is PTEN. Germline mutations of PTEN are found in patients with Cowden syndrome, which predisposes to breast and thyroid neoplasia. Recent evidences suggest that reduced expression of PTEN plays a crucial role in thyroid cancer [32-35]. Moreover, Frisk et al. have reported that PTEN inactivation is involved in highly malignant or late-stage thyroid cancer, especially anaplastic subtype [36]. Our results suggest that over-expression of miR-19a and miR-19b might be associated with translational suppression of PTEN and induce cell growth in ATCs.

We also found over-expression of miR-106a and miR-106b, and LNA-17-5p inhibited the expression of these homologous miRNAs. Since one of predicted target of these miRNAs is also E2F1 [31], suppression of them might result in cellular senescence by the above-mentioned mechanism. Moreover, we demonstrated that tumor suppressor RB1 was markedly up-regulated by LNA-17-5p. This is consistent with the report suggesting a post-transcriptional regulation of RB1 by miR-106a over-expression in colon cancer [37]. Therefore, up-regulation of RB1 by LNA-17-5p might result in a negative action in ATC proliferation.

When one or two of five miRNAs (miR-17-3p, miR-17-5p, miR-19a, miR-19b and miR-20a) were inhibited, the cell growth was significantly reduced in ATC cells. On the other hand, suppression of miR-18a only moderately reduced the cell growth. There is a possibility that this slight growth reduction was due to weak binding of LNA-18a to miR-17-5p or miR-20a. Although the expression of miR-17-5p and miR-20a was not changed after transfection with LNA-18a in Northern blot analysis that was done under denaturing condition, LNA-18a may weakly bind to miR-17-5p or miR-20a in physiological condition and inhibit their function in actual live cells.

Hayashita et al. have reported that the miR-17-92 cluster was over-expressed in the most aggressive form of lung cancer, small-cell cancer and might play a role in its development [10]. Very recently, Matsubara et al. have also demonstrated that inhibition of miR-17-5p and miR-20a caused apoptosis in lung cancer cells, whereas miR-18a and miR-19a did not show significant change in cell growth [38]. The function of each miRNA in the cluster seems to be dependent on type of cells. In ATC cells, downregulation of PTEN might be more important for cell growth as mentioned above.

In PTCs, two groups have concordantly reported that miR-221 and miR-222 are over-expressed and modulate KIT expression [12, 13]. However, in our microarray data, the expression of those miRNAs in ARO cells was conversely under-expressed. ARO cells harbor $BRAF^{V600E}$ mutation and are accordingly thought to originate from PTC [39], suggesting that those miRNAs may play a role in PTC carcinogenesis but are no longer

critical after anaplastic transformation.

In conclusion, our results demonstrate that the miR-17-92 cluster plays an important role in cell growth in some ATCs, and miR inhibitors containing LNA efficiently block cell proliferation and even induce cell death. The miR inhibitors against miR-17-92 cluster could be a novel therapeutic approach to certain types of ATCs.

Acknowledgements

This work was supported in part by Grant-in-Aid for Scientific Research (#18790637 and #18591030) and Global COE Program from the Ministry of Education, Culture, Sports, Science and Technology of Japan, the President's discretionary fund of Nagasaki University and Nagasaki Igakudousoukai fund for medical research.

References

1 Bartel DP. MicroRNAs: genomics, biogenesis, mechanism, and function. *Cell* 2004; **116**: 281-97.

2 Ambros V. MicroRNA pathways in flies and worms: growth, death, fat, stress, and timing. *Cell* 2003; **113**: 673-6.

3 Esquela-Kerscher A, Slack FJ. Oncomirs - microRNAs with a role in cancer. *Nat Rev Cancer* 2006; **6**: 259-69.

4 Calin GA, Croce CM. MicroRNA-cancer connection: the beginning of a new tale.

Cancer Res 2006; **66**: 7390-4.

5 Cimmino A, Calin GA, Fabbri M *et al.* miR-15 and miR-16 induce apoptosis by targeting BCL2. *Proc Natl Acad Sci U S A* 2005; **102**: 13944-9.

6 Takamizawa J, Konishi H, Yanagisawa K *et al.* Reduced expression of the let-7 microRNAs in human lung cancers in association with shortened postoperative survival. *Cancer Res* 2004; **64**: 3753-6.

7 Johnson SM, Grosshans H, Shingara J *et al.* RAS is regulated by the let-7 microRNA family. *Cell* 2005; **120**: 635-47.

8 Chan JA, Krichevsky AM, Kosik KS. MicroRNA-21 is an antiapoptotic factor in human glioblastoma cells. *Cancer Res* 2005; **65**: 6029-33.

9 He L, Thomson JM, Hemann MT *et al.* A microRNA polycistron as a potential human oncogene. *Nature* 2005; **435**: 828-33.

10 Hayashita Y, Osada H, Tatematsu Y *et al.* A polycistronic microRNA cluster, miR-17-92, is overexpressed in human lung cancers and enhances cell proliferation. *Cancer Res* 2005; **65**: 9628-32.

11 O'Donnell KA, Wentzel EA, Zeller KI, Dang CV, Mendell JT. c-Myc-regulated microRNAs modulate E2F1 expression. *Nature* 2005; **435**: 839-43.

12 He H, Jazdzewski K, Li W *et al.* The role of microRNA genes in papillary thyroid carcinoma. *Proc Natl Acad Sci U S A* 2005; **102**: 19075-80.

13 Pallante P, Visone R, Ferracin M *et al.* MicroRNA deregulation in human thyroid papillary carcinomas. *Endocr Relat Cancer* 2006; **13**: 497-508.

14 Weber F, Teresi RE, Broelsch CE, Frilling A, Eng C. A limited set of human MicroRNA is deregulated in follicular thyroid carcinoma. *J Clin Endocrinol Metab* 2006; **91**: 3584-91.

15 Visone R, Pallante P, Vecchione A *et al.* Specific microRNAs are downregulated in human thyroid anaplastic carcinomas. *Oncogene* 2007; **26**: 7590-5.

16 Ain KB. Anaplastic thyroid carcinoma: behavior, biology, and therapeutic approaches. *Thyroid* 1998; **8**: 715-26.

17 Vini L, Harmer C. Management of thyroid cancer. *Lancet Oncol* 2002; **3**: 407-14.

18 Fagin JA, Matsuo K, Karmakar A, Chen DL, Tang SH, Koeffler HP. High prevalence of mutations of the p53 gene in poorly differentiated human thyroid carcinomas. *J Clin Invest* 1993; **91**: 179-84.

19 Kurebayashi J, Otsuki T, Tanaka K, Yamamoto Y, Moriya T, Sonoo H.

Medroxyprogesterone acetate decreases secretion of interleukin-6 and parathyroid hormone-related protein in a new anaplastic thyroid cancer cell line, KTC-2. *Thyroid* 2003; **13**: 249-58.

20 Tanaka J, Ogura T, Sato H, Hatano M. Establishment and biological characterization of an in vitro human cytomegalovirus latency model. *Virology* 1987; **161**: 62-72.

21 Estour B, Van Herle AJ, Juillard GJ *et al.* Characterization of a human follicular thyroid carcinoma cell line (UCLA RO 82 W-1). *Virchows Arch B Cell Pathol Incl Mol Pathol* 1989; **57**: 167-74.

22 Kawabe Y, Eguchi K, Shimomura C *et al.* Interleukin-1 production and action in thyroid tissue. *J Clin Endocrinol Metab* 1989; **68**: 1174-83.

23 Muller PY, Janovjak H, Miserez AR, Dobbie Z. Processing of gene expression data generated by quantitative real-time RT-PCR. *Biotechniques* 2002; **32**: 1372-4, 6, 8-9.

24 Dimri GP, Lee X, Basile G *et al.* A biomarker that identifies senescent human cells in culture and in aging skin in vivo. *Proc Natl Acad Sci U S A* 1995; **92**: 9363-7.

25 Bulgin D, Podtcheko A, Takakura S *et al.* Selective pharmacologic inhibition of c-Jun NH2-terminal kinase radiosensitizes thyroid anaplastic cancer cell lines via induction of terminal growth arrest. *Thyroid* 2006; **16**: 217-24.

26 Chen C, Ridzon DA, Broomer AJ *et al.* Real-time quantification of microRNAs by stem-loop RT-PCR. *Nucleic Acids Res* 2005; **33**: e179.

27 Griffiths-Jones S, Grocock RJ, van Dongen S, Bateman A, Enright AJ. miRBase: microRNA sequences, targets and gene nomenclature. *Nucleic Acids Res* 2006; **34**: D140-4.

28 Trimarchi JM, Lees JA. Sibling rivalry in the E2F family. *Nat Rev Mol Cell Biol* 2002; **3**: 11-20.

29 Lazzerini Denchi E, Attwooll C, Pasini D, Helin K. Deregulated E2F activity induces hyperplasia and senescence-like features in the mouse pituitary gland. *Mol Cell Biol* 2005; **25**: 2660-72.

30 Ishigaki K, Namba H, Nakashima M *et al.* Aberrant localization of beta-catenin correlates with overexpression of its target gene in human papillary thyroid cancer. *J Clin Endocrinol Metab* 2002; **87**: 3433-40.

31 Lewis BP, Shih IH, Jones-Rhoades MW, Bartel DP, Burge CB. Prediction of

mammalian microRNA targets. *Cell* 2003; **115**: 787-98.

32 Weng LP, Brown JL, Eng C. PTEN coordinates G(1) arrest by down-regulating cyclin D1 via its protein phosphatase activity and up-regulating p27 via its lipid phosphatase activity in a breast cancer model. *Hum Mol Genet* 2001; **10**: 599-604.

33 Halachmi N, Halachmi S, Evron E *et al.* Somatic mutations of the PTEN tumor suppressor gene in sporadic follicular thyroid tumors. *Genes Chromosomes Cancer* 1998; **23**: 239-43.

34 Gimm O, Perren A, Weng LP *et al.* Differential nuclear and cytoplasmic expression of PTEN in normal thyroid tissue, and benign and malignant epithelial thyroid tumors. *Am J Pathol* 2000; **156**: 1693-700.

35 Bruni P, Boccia A, Baldassarre G *et al.* PTEN expression is reduced in a subset of sporadic thyroid carcinomas: evidence that PTEN-growth suppressing activity in thyroid cancer cells mediated by p27kip1. *Oncogene* 2000; **19**: 3146-55.

36 Frisk T, Foukakis T, Dwight T *et al.* Silencing of the PTEN tumor-suppressor gene in anaplastic thyroid cancer. *Genes Chromosomes Cancer* 2002; **35**: 74-80.

37 Volinia S, Calin GA, Liu CG *et al.* A microRNA expression signature of human solid tumors defines cancer gene targets. *Proc Natl Acad Sci U S A* 2006; **103**: 2257-61.

38 Matsubara H, Takeuchi T, Nishikawa E *et al.* Apoptosis induction by antisense oligonucleotides against miR-17-5p and miR-20a in lung cancers overexpressing miR-17-92. *Oncogene* 2007; **26**: 6099-105.

39 Namba H, Nakashima M, Hayashi T *et al.* Clinical implication of hot spot BRAF mutation, V599E, in papillary thyroid cancers. *J Clin Endocrinol Metab* 2003; **88**: 4393-7.

Figure legends

Figure 1. Expression of miRNAs in thyroid cancer cell lines. A, Northern blot for members of the miR-17-92 cluster. B, Northern blot for other cancer-related miRNAs. A and B, 5S ribosomal RNA (5S-rRNA) was used as a loading control. Similar results were obtained in at least two independent experiments. C, Real-time RT-PCR for miRNAs with highly similar sequence. The expression level of indicated miRNA was measured as described in Materials and Methods. U6 small nuclear RNA was used as an internal control. Each bar indicates the mean and standard error of the data collected in triplicate.

Figure 2: Expression of miR-17-3p and miR-17-5p in human ATCs. Real-time RT-PCR was performed using RNA from 6 human ATC tissues (filled bars) and paired normal tissues (empty bars). The expression level of indicated miRNA was measured as described in Materials and Methods. U6 small nuclear RNA was used as an internal control. Each bar indicates the mean and standard error of the data collected in triplicate.

Figure 3. Suppression of miRNAs by miR inhibitors. A and B, ARO cells were transfected with indicated miR inhibitors. Total RNA was extracted at indicated time points and subjected to Northern blot analysis using indicated probes. 5S-rRNA was used as a loading control. Similar results were obtained in at least two independent

experiments. C, alignments of homologous miRNAs are shown. Asterisk indicates mismatched base.

Figure 4: Effect of miR inhibitors on ATC cell growth. A and B, Time course curves. The indicated cells were transfected with indicated miR inhibitors (40 pmol/well) as described in Materials and Methods. The number of cells was counted at indicated times after initial transfection. *P<0.0001 vs. reagent only, LNA-18a and LNA-21. **P<0.0001 vs. reagent only and LNA-21. C, Dose-dependent curve. ARO cells were transfected with indicated dose of miR inhibitors (0~40 pmol/well) as described in Materials and Methods. The number of cells was counted at 72 hr after transfection (24 hr after second transfection). *P<0.01 vs. LNA-18a, LNA-19a and LNA-21. **P<0.0001 vs. LNA-21a. ***P<0.0001 vs. LNA-18a and LNA-21. A, B and C, Each point indicates the mean and standard deviation of three wells. Similar results were obtained in three independent experiments.

Figure 5: Effect of miR inhibitors on apoptosis in ARO cells. ARO cells were transfected with indicated miR inhibitors. A, Images were obtained at 72 hr after transfection (24 hr after second transfection). D2R and DRAQ-5 were excited with 488 and 633 nm laser, respectively. Representative images are shown. Nuclear fragmentation is indicated by arrowhead. UV exposure was used as a positive control. B, Cells were harvested at 72 hr after transfection (24 hr after second transfection), and Western blot was performed using indicated primary antibodies. β-actin was used as a

loading control. C, Agarose gel electrophoresis of DNA extracted from the cells used in B. Similar results were observed in three independent experiments.

Figure 6: Effects of miR inhibitors on cellular senescence in ARO cells. A, After SA-β-gal staining, the number of senescent cells was counted at 72 hr after transfection (24 hr after second transfection). Each bar indicates the mean and standard deviation of 10 fields. Similar results were obtained in at least two independent experiments. *P < 0.0001 vs. others. B, Representative images are shown. Enlarged and positively stained senescent cells are indicated by arrowheads. All images were obtained using a same magnification.

Figure 7: Effects of miR inhibitors on target protein expression. ARO cells were transfected with indicated miR inhibitors (400 pmol in 6 cm culture dish). Cells were harvested 96 hr after transfection, and Western blot was performed using indicated primary antibodies. β-actin was used as a loading control. Similar results were obtained at least two independent experiments.

Table 1. Expression pattern of miRNAs in ARO compared with PT

miRNA	Fold Change	miRNA	Fold Change
hsa-mir-192	16.53	hsa-let-7	1.02
hsa-mir-196a	11.95	hsa-mir-17-3p	0.98
hsa-mir-194	9.14	hsa-mir-21	0.88
hsa-mir-429	6.69	hsa-mir-145	0.70
has-mir-200b	6.28	hsa-mir-143	0.60
hsa-mir-7	6.18	hsa-mir-221	0.51
hsa-mir-10a	5.70	hsa-mir-210	0.40
hsa-mir-16	5.27	hsa-mir-222	0.40
hsa-mir-20a	3.37	hsa-mir-23a	0.34
hsa-mir-106b	3.26	hsa-mir-27a	0.30
hsa-mir-17-5p	2.25	hsa-mir-24	0.30
hsa-mir-106a	2.20	hsa-mir-199a	0.25
hsa-mir-19b	2.12	hsa-mir-148a	0.19
hsa-mir-18a	1.46	hsa-mir-100	0.19
hsa-mir-92	1.38	hsa-mir-138	0.08
hsa-mir-19a	1.29	hsa-mir-125b	0.05

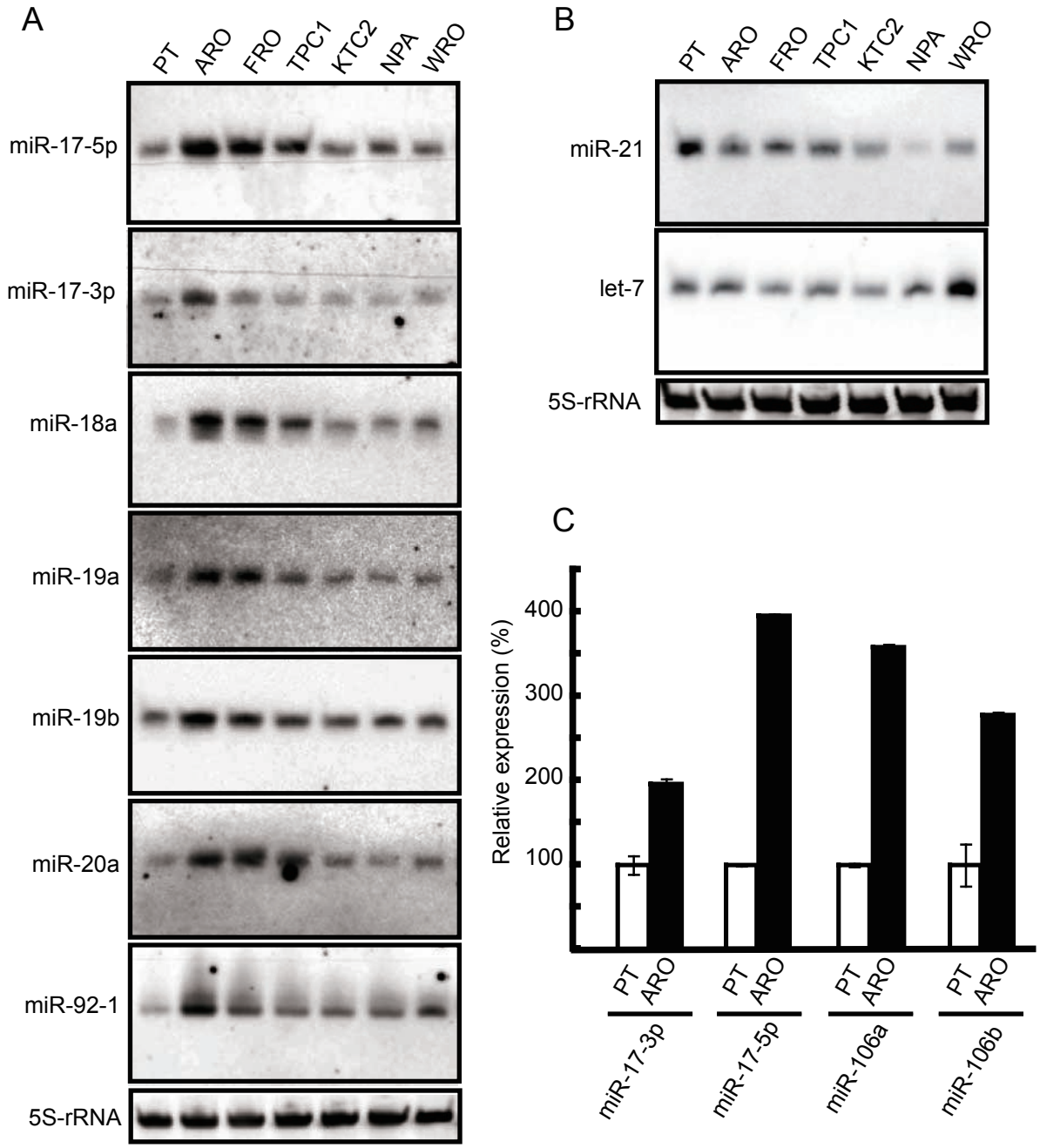
A
PT
ARO
FRO
TPC1
KTC2
NPA
WRO
miR-17-5p
miR-17-3p
miR-18a
miR-19a
miR-19b
miR-20a
miR-92-1
5S-rRNA
B
PT
ARO
FRO
TPC1
KTC2
NPA
WRO
miR-21
let-7
5S-rRNA
C
Relative expression (%)
400
300
200
100
PT
ARO
miR-17-3p
miR-17-5p
miR-106a
miR-106b

Figure 2

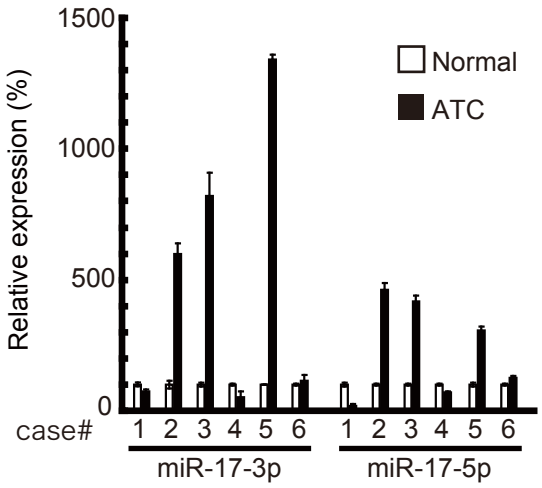
1500
1000
500
0
Relative expression (%)
Normal
ATC
case#
1 2 3 4 5 6
1 2 3 4 5 6
miR-17-3p
miR-17-5p

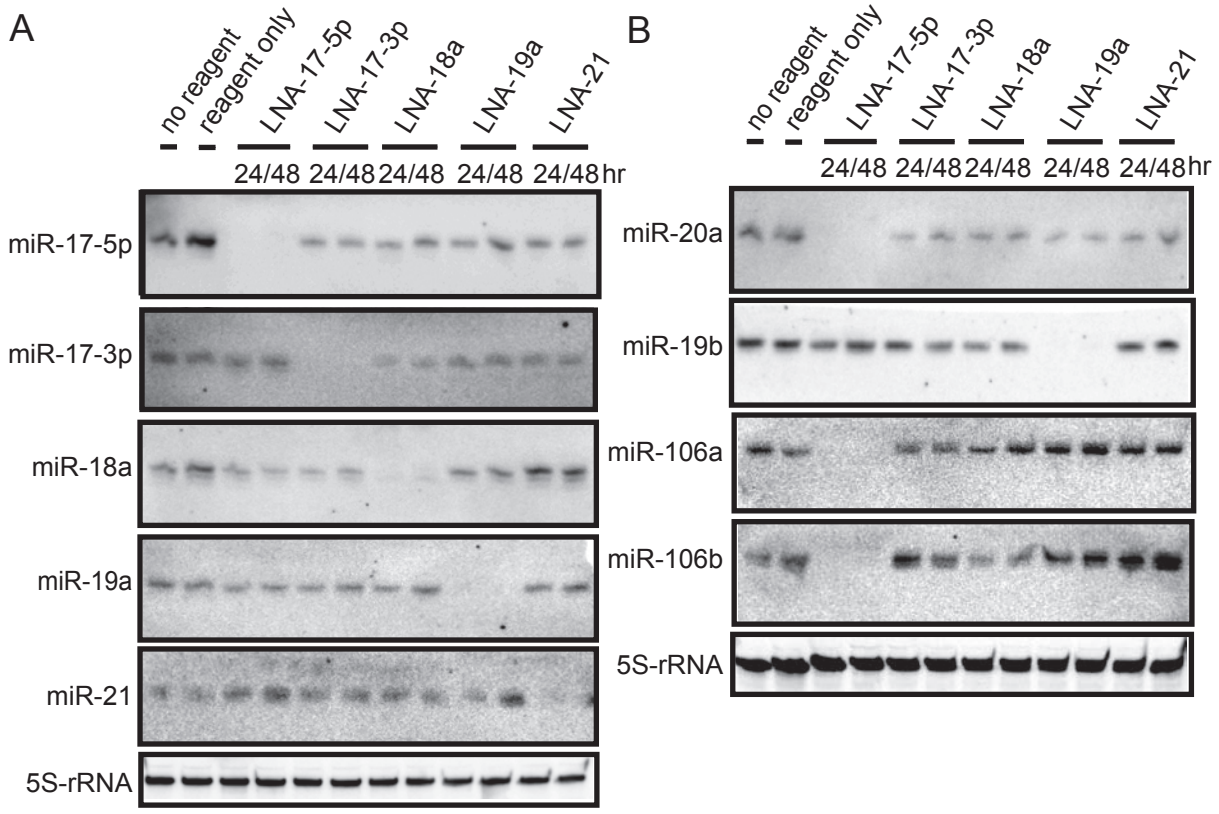

C

```
miR-17-5p  CAAAGUGCUUACAGUGCAGGUAGU
miR-20a    UAAAGUGCUUAUAGUGCAGGUAG

miR-17-5p  CAAAGUGCUUACAGUGCAGGUAGU
miR-18a    UAAGGUGCAUCUAGUGCAGAUA

miR-17-5p  CAAAGUGCUUACAGUGCAGGUAGU
miR-106a   AAAAGUGCUUACAGUGCAGGUAGC

miR-17-5p  CAAAGUGCUUACAGUGCAGGUAGU
miR-106b   UAAAGUGCUGACAGUGCAGAU

miR-20a    UAAAGUGCUUAUAGUGCAGGUAG
miR-18a    UAAGGUGCAUCUAGUGCAGAUA

miR-19a    UGUGCAAAUCUAUGCAAAACUGA
miR-19b    UGUGCAAAUCCAUGCAAAACUGA
```

Figure 4

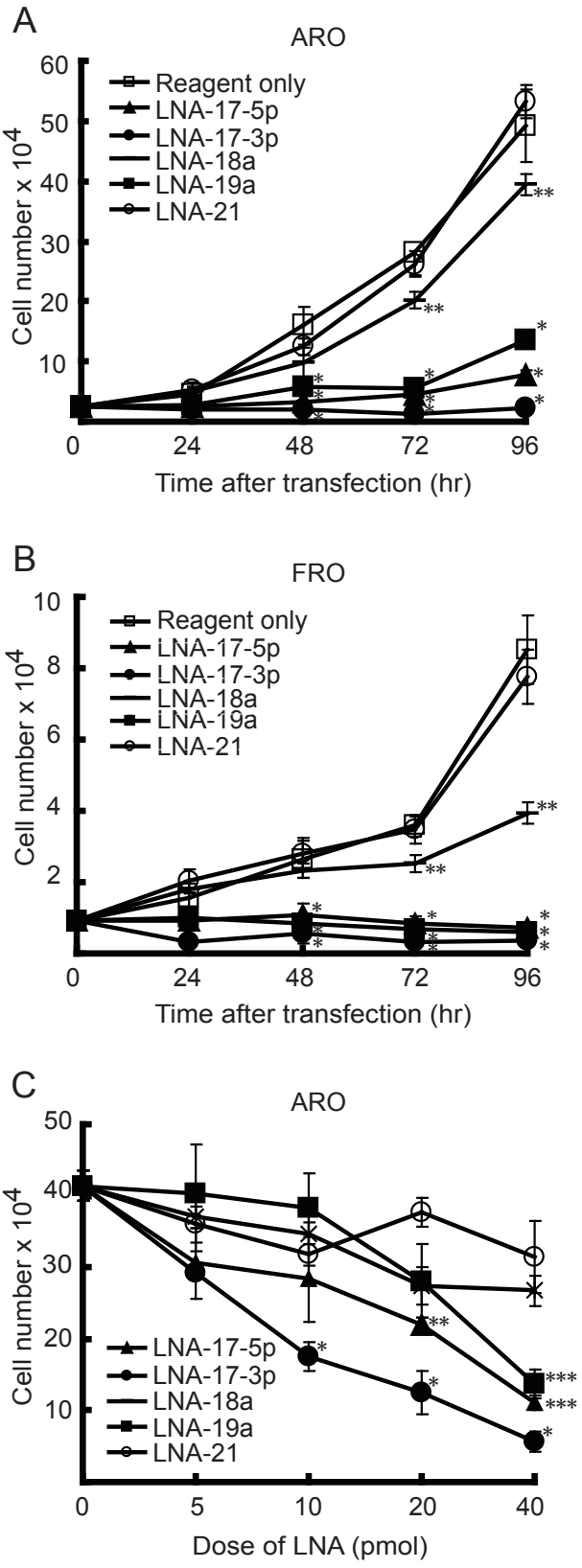
A
ARO
Reagent only
LNA-17-5p
LNA-17-3p
LNA-18a
LNA-19a
LNA-21
Cell number x 10^4
Time after transfection (hr)
B
FRO
C
ARO
Dose of LNA (pmol)

Figure 5

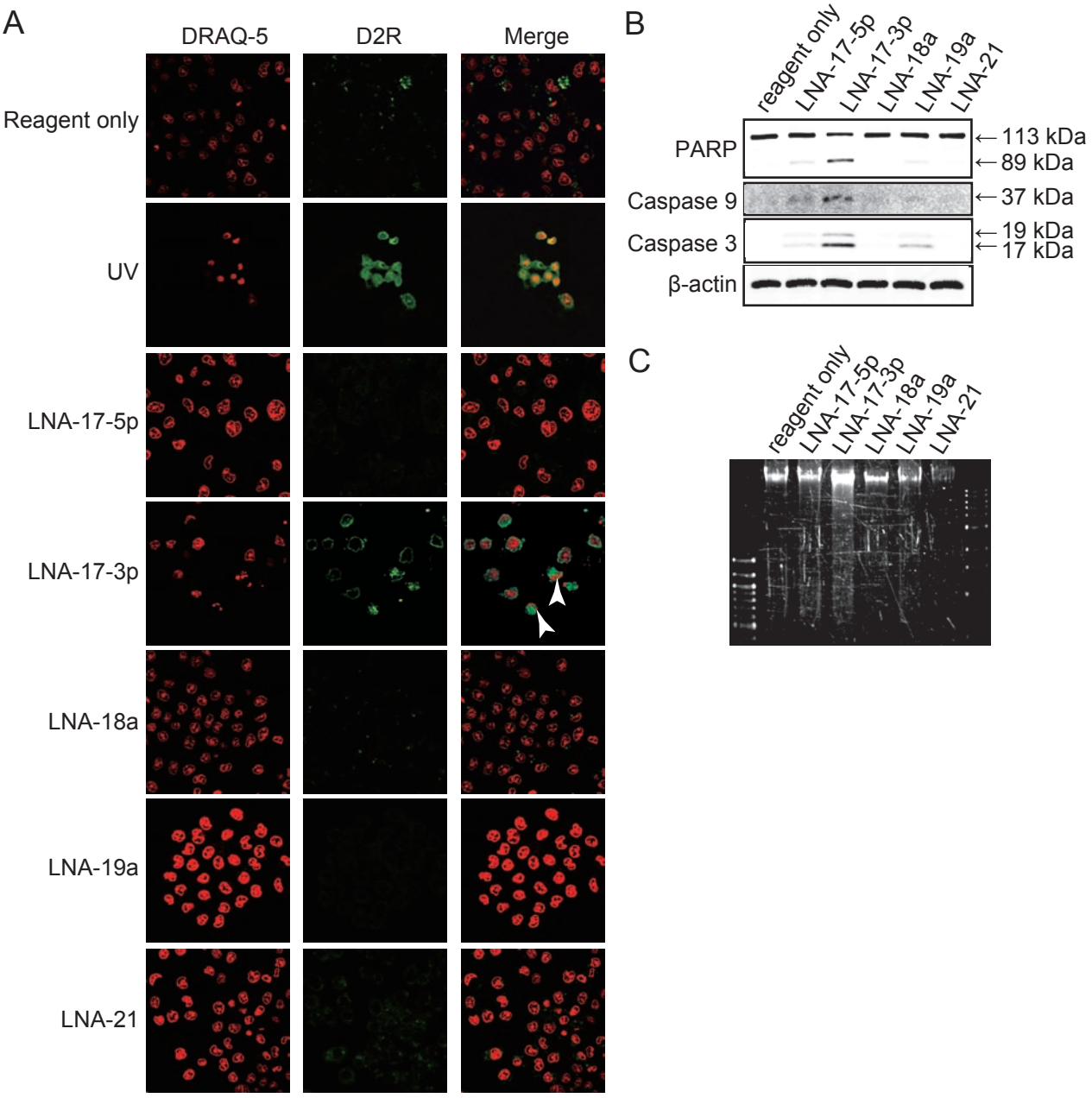
A
DRAQ-5
D2R
Merge
Reagent only
UV
LNA-17-5p
LNA-17-3p
LNA-18a
LNA-19a
LNA-21
B
reagent only
LNA-17-5p
LNA-17-3p
LNA-18a
LNA-19a
LNA-21
PARP
Caspase 9
Caspase 3
β-actin
113 kDa
89 kDa
37 kDa
19 kDa
17 kDa
C
reagent only
LNA-17-5p
LNA-17-3p
LNA-18a
LNA-19a
LNA-21

Figure 6

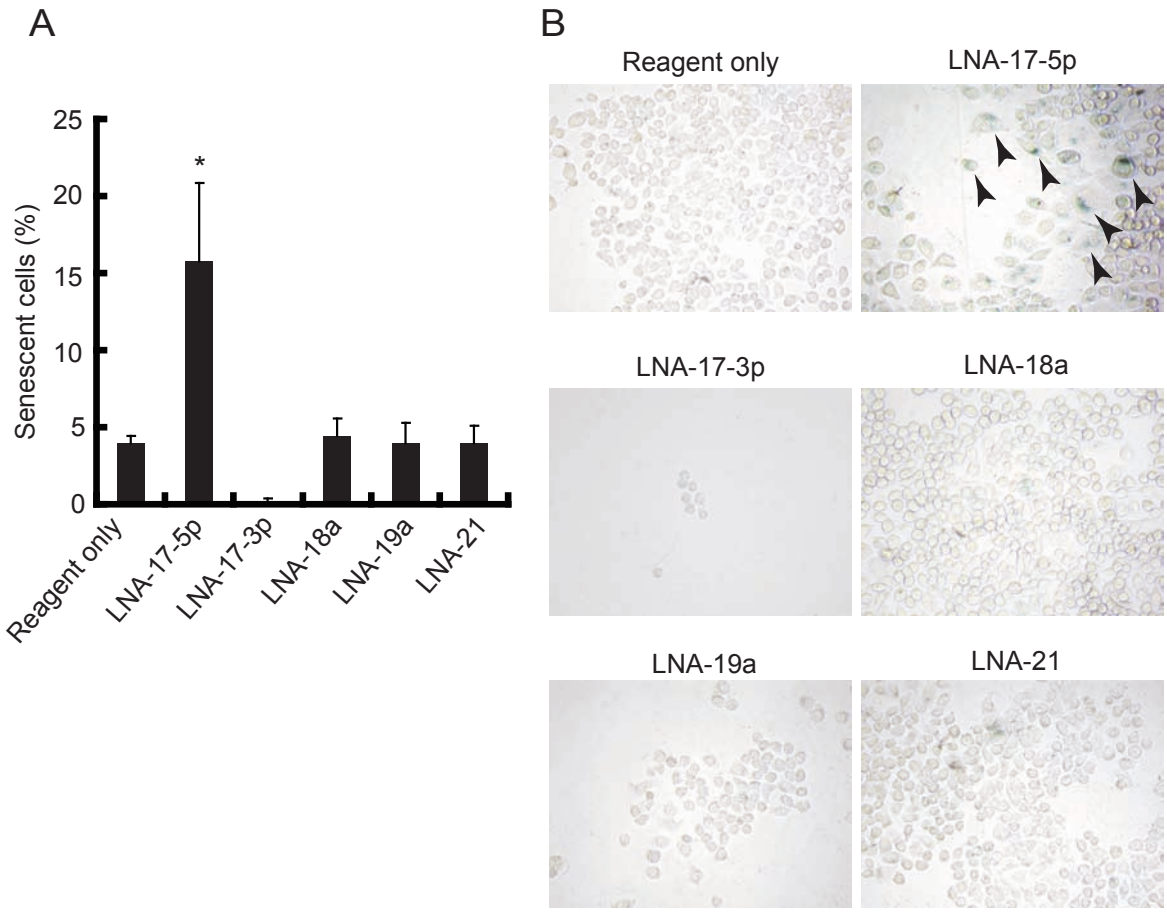
A
B
Senescent cells (%)
25
20
15
10
5
0
*
Reagent only
LNA-17-5p
LNA-17-3p
LNA-18a
LNA-19a
LNA-21
Reagent only
LNA-17-5p
LNA-17-3p
LNA-18a
LNA-19a
LNA-21

Figure 7

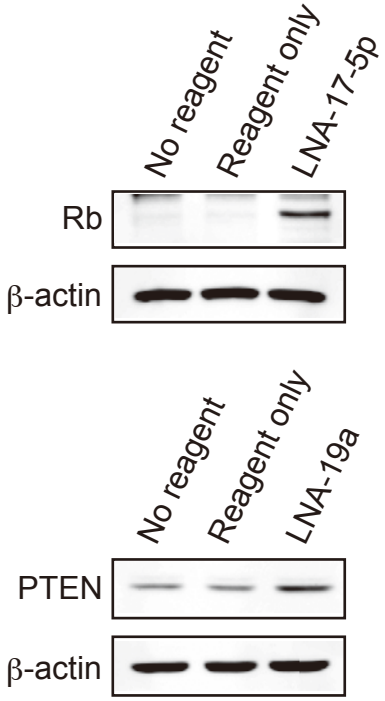
No reagent
Reagent only
LNA-17-5p
Rb
β-actin
No reagent
Reagent only
LNA-19a
PTEN
β-actin